Electrode Concepts for High Capacity Conversion Type Battery Electrodes

A thesis submitted towards the partial fulfilment of BS-MS programme

By

Anjana Raj R

20121073

Department of Chemistry

Indian Institute of Science Education and Research (IISER), Pune, India.

Under the guidance of

Dr. Stefan. A. Freunberger

Department of Chemistry,

Institute for Chemistry and Technology of Materials (ICTM), Graz, Austria.

Certificate

This is to certify that this dissertation entitled "***Electrode Concepts for High Capacity Conversion Type Battery Electrodes***" towards the partial fulfilment of the BS-MS dual degree program at the Indian Institute of Science Education and Research, Pune represents original research carried out by "Anjana Raj R at the Institute for Chemistry and Technology of Materials, Graz, Austria" under the supervision of "Dr. Stefan. A. Freunberger, Department of Technical Chemistry, Process technology and Biotechnology" during the academic year 2016-2017.

Stefan Freunberger

Date: 20/03/2017

Place: Graz

Dr. Stefan. A. Freunberger

Department of Chemistry,

ICTM, Graz, Austria.

Dedicated to my family & friends

Declaration

I hereby declare that the matter embodied in the report entitled "***Electrode Concepts for High Capacity Conversion type Battery Electrodes***" are the results of the investigations carried out by me at the Department of Chemistry, Institute for Chemistry and Technology of Materials, Graz, Austria, under the supervision of Dr. Stefan. A. Freunberger and the same has not been submitted elsewhere for any other degree.

Date: 20/03/2017

Anjana Raj R

Place: Graz, Austria

Acknowledgements

I would like to express my sincere gratitude to my supervisor, Dr. Stefan. A. Freunberger for his excellent guidance and giving me an opportunity to do my Master project with his working group in ICTM, Graz.

I sincerely thank all my lab mates especially Bettina Schafzahl who rendered her help and valuable suggestions during my entire project work to carry out the experiments with utmost care.

I really thank each and every one in ICTM for helping me to carry out the project by making me more comfortable in an entirely new atmosphere.

I would also like to acknowledge my TAC member Dr. Muhammed Musthafa, IISER Pune who motivated and encouraged me to complete the project successfully.

Finally I would like to thank my family & friends for their valuable support during my entire project.

Table of Contents

List of Figures

List of Tables

Abstract

Li-O_2 batteries have become a promising candidate in the scientific world and can be a better replacement for the existing energy storage devices because of their theoretical high specific capacity. However, they suffer from poor rechargeability, high charging voltages, low efficiency, accumulation of side products like Li_2CO_3, HCOOLi etc. Here, we tried to study the possible mechanisms that can occur during their cycling and also the parasitic reactions associated with it. We found from the pressure measurements that the disproportionation reaction occurs during charge in addition to discharge. Moreover, the number of e^- per mole of O_2 deviate from the ideal value of 2 because of the parasitic reactions and many other factors still unknown. A method based on Mass Spectrometry has been developed to quantify those carbonaceous side products along with the discharge products for Li-O_2 and Na-O_2 batteries. Based on that method, discharge products like Li_2O_2, NaO_2 and KO_2 can be quantitatively determined using aq.$FeCl_3$ and side products with the acid and Fenton's reagent. But there many factors still unknown about this method like the reactivity of different ions in the solutions.

Introduction

The electrification of transportation can reduce the consumption of fossil fuels and the consequences caused by them such as CO_2 emission, climate change and air pollution. For the complete electrification of road transport, developing a cost-effective, safe and environmentally benign secondary batter is important. This should possess sufficient specific energy and energy density. Many vehicles like hybrid electric vehicles (HEV), plug in electric vehicles (PHEV) etc. which are all based on Li-ion battery technology are already in serial production. But such batteries are not capable enough for the complete electrification of road transport. This led to a situation that a new battery chemistry with a theoretical specific energy and energy density surpassing that of the current Li-ion is needed. These type of batteries are often referred to as “beyond Li-ion” (BLI). Among those, Li-air batteries gained tremendous attention in the scientific world due to their high theoretical specific energy (~3500Wh kg^{-1}) and energy density (~3445Wh L^{-1})[1-5].

1.1. Li-O_2 Battery

Li-O_2 battery is a promising candidate among all the other metal-air battery systems because of its high theoretical specific energy and energy density. It has the potential of 2-4 times the specific energy of a Li-ion battery and a comparable theoretical specific energy with that of gasoline. As many factors are still unknown about these batteries, the values of practical specific energies are unclear. But batteries with specific energy in the range of 500-1000 Wh kg^{-1} can run an electric vehicle up to 500 Km. The practical specific energy of some rechargeable batteries is shown in Fig.1a.There are 4 types of Li-O_2 batteries: aqueous, non-aqueous, hybrid and solid state batteries.

A typical aqueous and non-aqueous Li-O_2 battery consists of a Li metal negative electrode, a porous positive electrode and a Li^+ conducting electrolyte. The key electrochemical reaction that occurs in a non-aqueous Li-O_2 battery is $2Li_{(s)} + O_{2\,(g)} \leftrightarrow Li_2O_{2(s)}$ ($E^\circ_{Li_2O_2}$ = 2.96 V vs Li/Li^+). $E^\circ_{Li_2O_2}$ in this case is the standard electrode potential of bulk Li_2O_2 formation calculated using the Nernst equation.

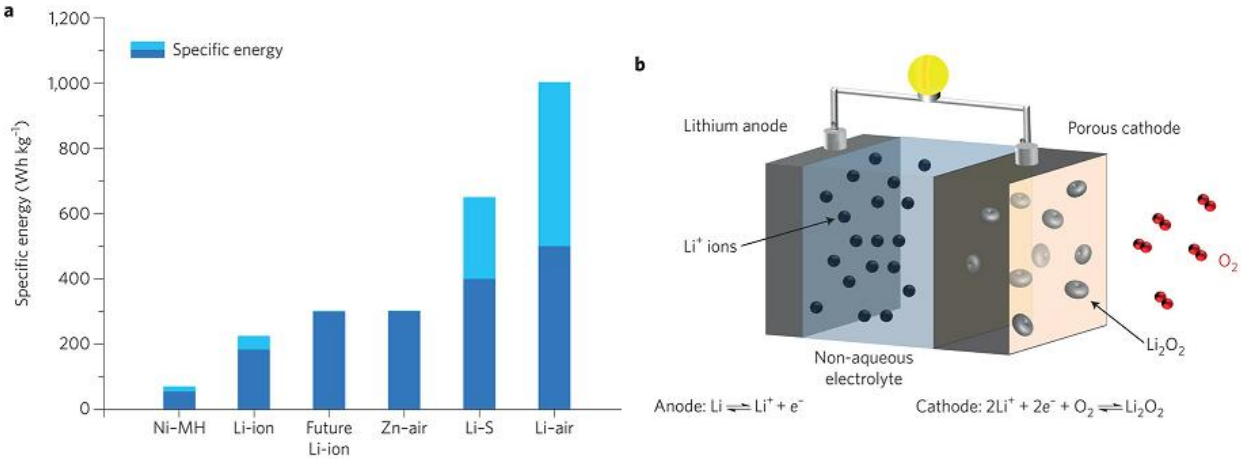

Fig.1.a.Projected practical specific energies for some rechargeable batteries. These are reduced from the theoretical values by, for example, current collectors, cell packaging and system overheads. Light blue indicates range of specific energies. b. Schematic of an aprotic Li–O_2 cell [5].

During discharge, O_2 at the cathode is reduced to O_2^{2-} and combines with Li^+ from the electrolyte to form Li_2O_2, which is the main discharge product and the reverse reaction occurs during charge. In the case of aqueous Li-O_2 battery, during discharge the Li^+ ion that gets oxidised at the anode reaches the cathode through the aqueous electrolyte and combine with the OH^- ions to form LiOH as follows: $2Li^+ + ½O_2 + H_2O + 2e^- \leftrightarrow 2LiOH$ (3.45 V vs Li/Li^+). During charge, LiOH reacts back. LiOH can prevent the air cathode from blocking and reaching high overpotentials because it is soluble in the aqueous electrolyte. The existence of the highly reactive Li metal in aqueous environment is problematic. The presence of a surface coating like LISICON ($Li\,M_2\,(PO_4)_3$, $Li_{1+x+y}\,Al_xTi_{2-x}Si_yP_{3-y}O_{12}$) can minimize this problem to an extent but this cannot provide a long-term protection from the Li-dendrite formation and pH variation and finally, can affect the rate

performance. The slow decomposition of LiOH can decrease the energy density and cyclability [5-11].

The hybrid Li-O_2 battery was introduced by combining the advantages of both aqueous and non-aqueous batteries. The aqueous cathode and the anode which is only in contact with the non-aqueous electrolyte are connected by a Li-ion conducting membrane. The combination of both types of electrodes can be done with a solid state electrolyte. But the components in the electrolyte can react with the metallic Lithium. A solid state Li-O_2 battery consists of a Li anode, porous carbon cathode and a glass, ceramic or glass-ceramic electrolyte. Even though it is safe and avoid the chance of ignition from rupture, the drawback of this battery is the low Li^+ ionic conductivity. This has led to giving more importance to the non-aqueous Li-O_2 battery in the recent years.

1.2. The non-aqueous Li-O_2 battery

The non-aqueous Li-O_2 battery was first reported by Abraham and Jiang in 1996.The use of an O_2 molecule from the air as an active material leads to a drastic improvement in the energy density. Here, the Li anode and the porous carbon cathode are separated by a non-aqueous electrolyte. During discharge, the anode Li loses an e^- and becomes Li^+ and combines with the reduced oxygen at the cathode to give the main discharge product, Li_2O_2 .The discharge product can be stored within the voids of the porous carbon electrode. Even though LiO_2 is formed as an intermediate in Li-O_2 batteries, it is unstable at room temperature and immediately gets converted to Li_2O_2 via disproportionation or charge transfer (eqn.3 & 4). The schematic diagram of a non-aqueous Li-O_2 battery is shown in Fig.1b.The mechanism proposed theoretically is

$$2\,Li \leftrightarrow 2\,(Li^+ + e^-) \qquad \text{(anode)} \qquad (1)$$

$$Li^+ + e^- + O_2^* \leftrightarrow LiO_2^* \qquad \text{(cathode)} \qquad (2)$$

$$Li^+ + e^- + LiO_2^* \leftrightarrow Li_2O_2^* \qquad \text{(cathode)} \qquad (3)$$

$$LiO_2^* + LiO_2^* \leftrightarrow Li_2O_2^* + O_2 \quad \text{(cathode)} \qquad (4)$$

where * refers to a surface-adsorbed species. Here the forward and reverse reaction represents the discharge and charge processes respectively. The electrically insulating nature of the discharge product can lead to high over potentials during charge [4-5].

Despite the promising factors regarding a Li-air battery, there are many challenges to overcome for its successful practical implementation. Perhaps the most significant obstacle arises from severe parasitic reactions during cycling. These reactions decompose the electrolyte as well as the porous electrode (typically carbon with binder) and cause poor rechargeability, high charging voltages, low efficiency, the buildup of parasitic side products, and early cell death within a few cycles. True reversibility of the cathode reaction in the Li-O_2 cell requires a set of quantities to obey the stoichiometry and to match each other during discharge and subsequent charge. These are

1) $e^-/O_2 = 2$ both on discharge and charge.

2) to produce exactly one mole of Li_2O_2 per one mole of O_2 and 2 e^- on discharge and the reverse on charge.

3) Absence of any other gas evolution, e.g. CO_2, or generation of solid products other than Li_2O_2 during discharge and charge and

4) O_2 consumed during discharge matches the amount released on the subsequent charge. Typically these measures deviate more or less significantly from the ideal due to parasitic reactions, which are not entirely understood.

The aim of my work was to further develop analysis techniques to quantify these measures. In particular two techniques are considered: First, measuring O_2 consumption and evolution with high accuracy and high speed (see point 1&4 above). Second, further developing a method to quantify the Li_2O_2 present and solid inorganic as well as organic parasitic products in the electrode at any stage of cycling (see point 2 & 3 above). These techniques shall be applied to help research work on topics ranging from (i) higher capacity cathodes using graphene based electrode materials, (ii) mechanistic

investigations of the role of disproportionation reactions during discharge and charge, (iii) influence of reactive oxygen species during cycling.

1.3. Na-O_2 battery

After developing the analysis techniques necessary for the determination of discharge product for Li-O_2 battery, we tried to expand this method to superoxides (KO_2 and NaO_2).The Na-O_2 battery is also another promising candidate among the metal-air batteries. It can be used as an alternative for Li-O_2 batteries. The key electrochemical reaction in a Na-O_2 battery is $Na^+ + e^- + O_2 \leftrightarrow NaO_2$, E^o=2.27 V vs Na/Na^+. Unlike in the case of a Li-O_2 battery, here a 1 e^-/O_2 process leads to NaO_2 as the main discharge product. The formation of a sodium superoxide (NaO_2) is more kinetically favored than a sodium peroxide (Na_2O_2).The presence of an abundant, feasible element like Na, better rechargeability and a much lower overpotential makes this battery more acceptable even though it possesses a low theoretical energy density (1105 $Whkg^{-1}$) compared to the Li-O_2 battery. The formation of a more stable discharge product (NaO_2) is responsible for the difference in electrochemical characteristics between these batteries [12-16].

Methods

2.1. Experimental section

Chemicals:

H_2O_2(30% v/v), $KMnO_4$ (99%), HCl(37% v/v), Bis(trifluoromethane)sulfonimide tetrabutylammoniumsalt(TBATFSI,>99%),Li_2CO_3(99.99%,Dimethylsulfoxide(DMSO,99.9 %) and 1,2- dimethoxyethane (DME, 99%) were purchased from Sigma-Aldrich®. Tetrabutylammonium perchlorate ($TBAClO_4$, >99.0%), 1, 4– diazabicyclo [2.2.2] octane (DABCO, Reagent Plus®, ≥99%), $FeSO_4.7H_2O$ (99%) were purchased from Fluka, Bis (trifluoromethane) sulfonamide lithium salt (LiTFSI, 99+ %) from Solvionic, H_3PO_4 (85% v/v) from Merck, Sodium acetate (NaOAc, 99%) and Potassium Superoxide (KO_2, 96.5%) from Alfa Aesar. DME was purified by distillation. Solvents used as electrolytes were dried over activated molecular sieves (4A°). All other chemicals were used without further purification. DABCO was purified via recrystallization from absolute diethyl ether. Li_2O_2 was synthesized according to a previously reported procedure[18].

- For Pressure measurements, Carbon cathodes were prepared with Super P and PTFE (10% in H_2O) binder using isopropyl alcohol as a solvent. The slurry was coated on an AV Carbon paper of 17 mm diameter. These were dried in vacuum at 170°C for 12-15 hours and subsequently they were transferred into an Argon filled glove box without exposure to air. Each electrode contains nearly 2 mg of the active material and the pressure cells were assembled with 270 µl electrolyte. $LiFePO_4$ was used as the counter electrode and has a potential of 3.45 V. Whatman Glass microfiber filters dried under vacuum at 180°C overnight were used as separators. The electrolytes used are
    1) 10 mM LiTFSI 90 mM TBATFSI in Monoglyme
    2) 10 mM LiTFSI 90 mM $TBAClO_4$ with and without 0.5 M DABCO in DMSO.

❖ Mass spectrometry measurements were carried out with known amounts of Li_2O_2, NaOAc, Li_2CO_3 and HCOOLi to find out the amount of O_2, inorganic and organic CO_2 evolving. We mechanically prepared mixtures of Li_2O_2 with Li_2CO_3 and HCOOLi and these were treated with 0.1 M aq.$FeCl_3$, 0.5 M $FeSO_4$ in 20% H_3PO_4 and 30% H_2O_2. For Na-O_2 battery, we prepared mixtures of KO_2 and NaOAc and treated with the same solutions as above.

❖ We also tried the permanganometric oxidation of the organic side product like HCOOLi with an acidic solution of 0.5 M $KMnO_4$ instead of the Fenton's reagent.

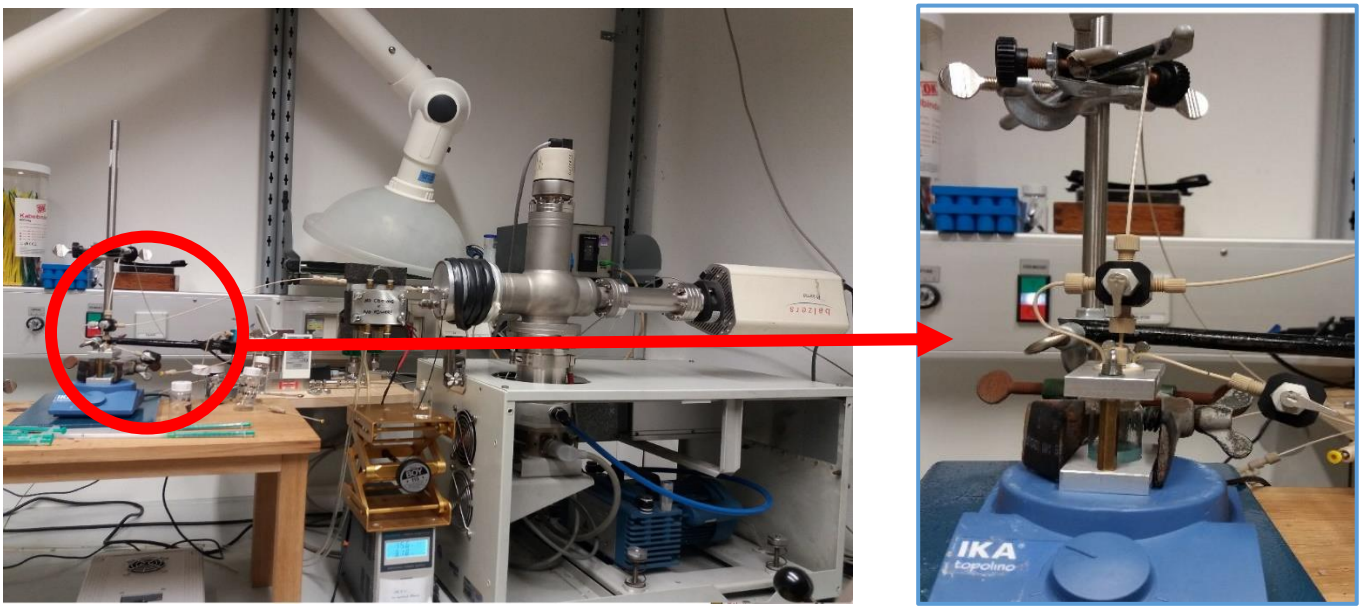

Fig.2. Image of a Mass Spectrometer and its setup

2.2. **Theoretical Section**

➢ Quantification of Li_2O_2 and different side products

A method had previously been developed to quantify parasitic products (Li_2CO_3 and organic products such as lithium carboxylates) in a Li-O_2 cathode by means of mass spectrometry. It involves treating the washed electrodes with acid to decompose the Li_2CO_3 present, followed by treatment with Fenton's reagent to oxidize the lithium carboxylates. The evolved CO_2 was quantified by mass spectrometry (MS). It would be highly desirable to also quantify in the same electrodes the amount of Li_2O_2 present. Some researchers have proposed methods to quantify Li_2O_2 by means of iodometric titration and photometric determination of the Ti^{4+} complex. However, they are plagued by systematic errors like decrease of yield due to O_2 evolution. We developed a method based on MS to quantify Li_2O_2 and different side products. The key step is to first evolve all the O_2 present in the Li_2O_2 via H_2O_2, without forming reactive oxygen species (ROS) [17-25].

The method for the decomposition of Li_2O_2 with a catalytic amount of aq.$FeCl_3$ was developed based on the Kremer-Stein Mechanism [26-27].

$$Fe^{3+} + H_2O_2 \longleftrightarrow [Fe^{III}OOH]^{2+} + H^+ \longleftrightarrow [Fe^{V}O]^{3+} + H_2O$$

$$[Fe^{V}O]^{3+} \xrightarrow{+H_2O_2} Fe^{3+} + H_2O + O_2$$

Here we can see a 2 electron oxidation of Fe^{3+} and 1 mole of O_2 has evolved from the decomposition of 2 moles of H_2O_2. By taking Kremer-Stein mechanism as a basis, we developed a method to quantify Li_2O_2 with 0.1 M aq.$FeCl_3$.The O_2 evolved during the decomposition was determined with the help of Mass Spectrometry.

$$2\ Li_2O_2 + Fe^{3+} + 2\ H_2O \longrightarrow O_2 + 4\ LiOH + Fe^{3+}$$

The decomposition of 2 moles of Li_2O_2 gives 1 mole of O_2.

We have expanded the method based on Kremer-Stein mechanism for the quantification of the discharge product of the Na-O_2 battery (NaO_2). Here we have taken KO_2 as an alternative to NaO_2 because it is easier to handle.

$KO_2 + Fe^{3+} \longrightarrow ¾\ O_2$

The decomposition of one mole of KO_2 results in the formation of ¾ mole of O_2 [28].

The quantification of inorganic side product like Li_2CO_3 was carried out with the help of H_3PO_4.

$3\ Li_2CO_3 + 2\ H_3PO_4 \longrightarrow 2\ Li_3(PO_4) + 3\ CO_2 + 3\ H_2O$

The decomposition of 1 mole of Li_2CO_3 gives 1 mole of CO_2.

We tried two methods for the quantitative determination of organic side product.

- Fenton's reagent (Fe^{2+} and H_2O_2)
- $KMnO_4$

- **Reaction with Fenton's reagent**

$Fe^{2+} + H_2O_2 \longrightarrow Fe^{3+} + OH^- + \cdot OH$ (1)

$Fe^{3+} + H_2O_2 \longrightarrow Fe^{2+} + \cdot OOH + H^+$ (2)

Disproportionation of H_2O_2 gives two different types of oxygen radicals – hydroxyl ($^{\bullet}OH$) and hydroperoxyl ($\cdot OOH$).These can oxidise the organic compounds to CO_2 and H_2O [18]. Even though there is a possibility of Eqn.2 the rate of this reaction was very low under normal conditions compared to Eqn.1.Eqn.2 can dominate during the photo Fenton's reaction i.e. in the presence of ultraviolet light.

$HCOOLi + Fe^{2+} + H_2O_2 \longrightarrow CO_2 + H_2O + LiOH + Fe^{3+}$

❖ **Reaction with acidic $KMnO_4$**

The highly oxidative nature of $KMnO_4$ was utilised for the quantitative determination of organic side product like HCOOLi. Here we have prepared a 0.5 M $KMNO_4$ solution in 2 M H_3PO_4 because the oxidizing effect of $KMnO_4$ is maximum in acidic medium.

$3HCOOLi + 2KMnO_4 + H_3PO_4 \longrightarrow 3CO_2 + 2MnO_2 + 3LiOH + H_2O + K_2HPO_4$

$3HCOOLi + KMnO_4 \longrightarrow 3CO_2$

The decomposition of 1 mole of HCOOLi gives 1 mole of CO_2.To quantify the inorganic and the organic side products, the amount of inorganic and organic CO_2 evolution was determined using MS.

➢ Pressure measurements

The volume changes in an electrochemical reaction become significant due to the participation of gaseous species. Therefore, the volume changes help to identify the chemical processes taking place during cycling. Due to practical reasons, it is easier to measure the change in pressure by keeping the volume constant. The pressure measurements were carried out with Li-O_2 batteries to find out the possible mechanism responsible for discharge and charge and also to study the parasitic reactions. In either case were to measure the number of moles of electron per mole of oxygen upon cycling. The electron per oxygen ratio is ideally 2 if Li_2O_2 is the only product consumed/ evolved during the electrochemical reactions. Several researchers have reported that the e^-/O_2 ratio significantly deviates from 2 during charging for various solvents, cathode materials and conducting salts. By measuring the e^-/O_2 ratio, we can quantify the contribution of side reactions.

The number of moles of O_2 evolved/consumed can be calculated from the change in pressure using the Ideal Gas Law.

No: of moles of O_2, n (O_2) = PV/RT

(Where V is the volume of gas in Litres, R (Universal gas constant) =8.314 J/mol. K, T is the absolute temperature in K, P is the absolute pressure in Pascal).

No: of moles of electron, n (e^-) = Q / F

(Where Q is the total electric charge passed through the substance in Coulombs, F is the Faraday constant = 96485 C/mol) [29-30].

Results and Discussion

3.1. Pressure measurements

Several pressure measurements were carried out with Li-O_2 batteries in various solvents like DMSO, Dimethoxy ethane (DME) to find out the possible mechanism responsible for discharge and charge and to study the parasitic reactions in the presence and absence of additives like DABCO. This will help to know the type of intermediate formed during discharge. In either case the aim is to measure the number of electron per mole of oxygen upon cycling and the presence of additives will remove the singlet oxygen if present.

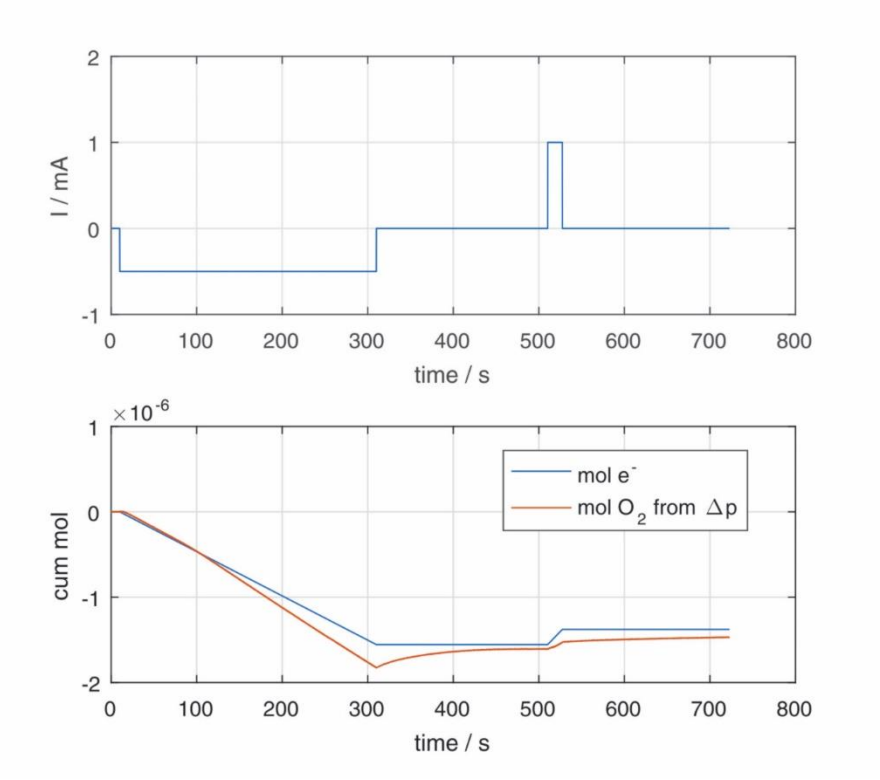

Fig.3.a) current profile b) the cumulative moles of electrons and oxygen molecule during discharge-charge of Li-O_2 cells with Dimethoxyethane as the solvent.

Particularly, current interrupt measurements with subsequent open circuit periods allow determining disproportionation reactions, Fig. 3(a), 4(a), 5(a). In all the measurements a discharge was followed by a resting period and charge. While disproportionation reactions ($2\ LiO_2 \rightarrow Li_2O_2 + O_2$) were known to occur on discharge, we could now clearly show that these also occur during charge, Fig. 3(b), 4(b), 5(b).Here we can see that even after the current becomes zero after the charge there was an increase in the cumulative moles of O_2 from Δp which indicates the disproportionation reaction.

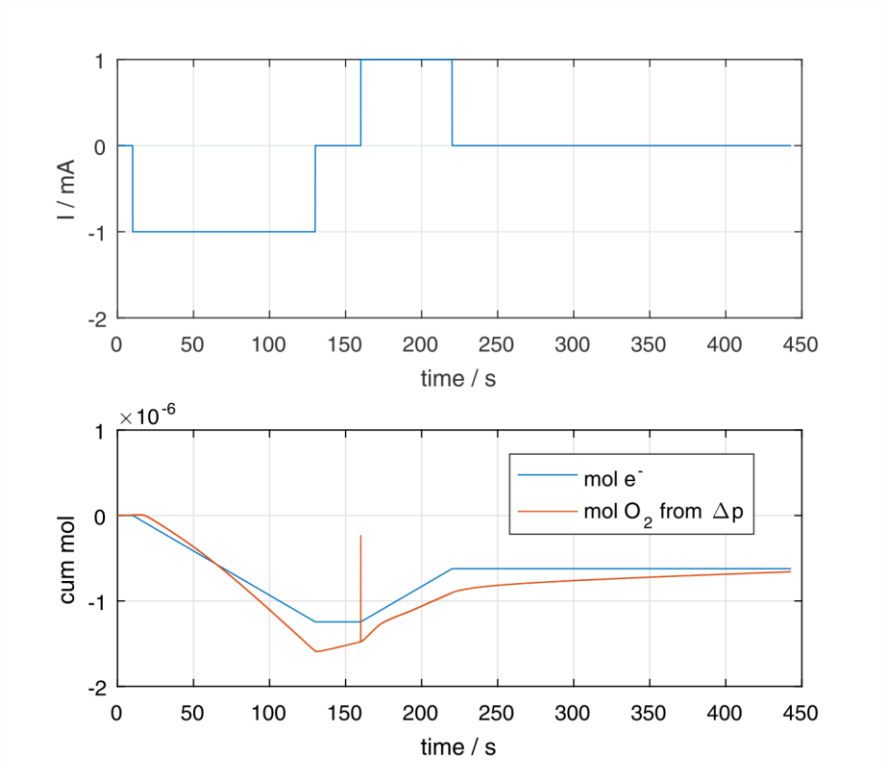

Fig.4.a) current profile b) the cumulative moles of electrons and oxygen molecule during discharge - charge of Li-O_2 cells with DMSO as the solvent.

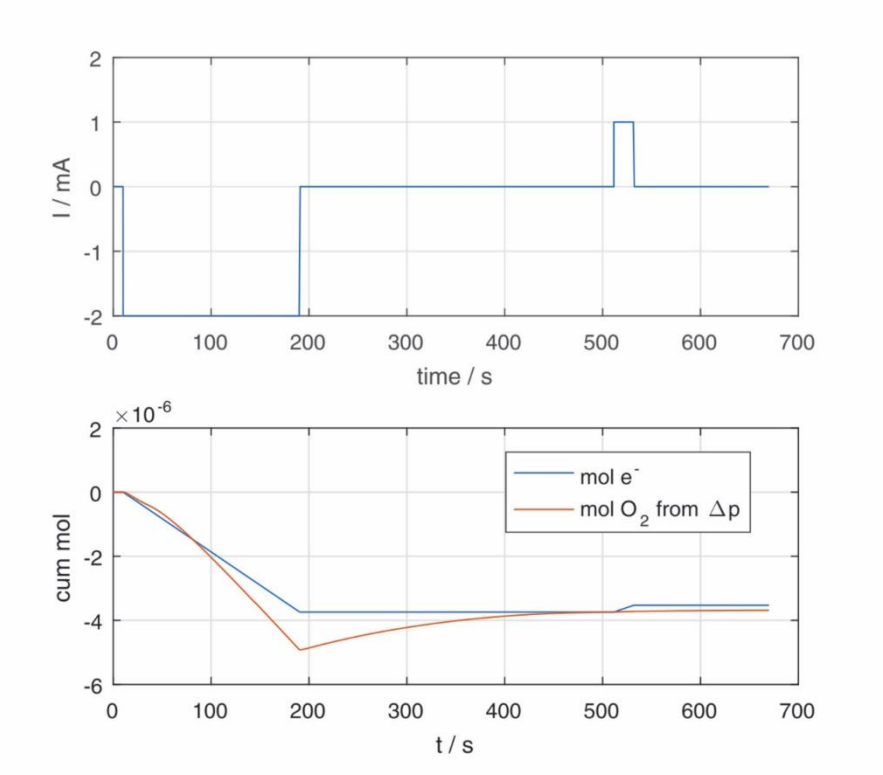

Fig.5.a) current profile b) the cumulative moles of electrons and oxygen molecule during discharge-charge of Li-O_2 cells with DMSO as the solvent in the presence of DABCO.

Then we tried to study the behavior in the presence of additives like DABCO (Fig.5.). However, we have not seen much difference in the presence of DABCO. Further work will more closely investigate the impact of the electrolyte on the charging mechanism including the role of disproportionation reactions. To do so, a numerical model needs to be developed to more clearly separate capacitive and Faradaic currents.

3.2. MS measurements

A new method based on MS has been developed for the quantification of the discharge products and the side products generated in the Li-O_2 and Na-O_2 batteries. The discharge products like Li_2O_2 and KO_2 were analysed with aq.$FeCl_3$ and the reaction results in the

evolution of O_2 while the side products like Li_2CO_3, HCOOLi, NaOAc etc. were with acid, permanganometric method and Fenton's reagent results in the evolution of CO_2.

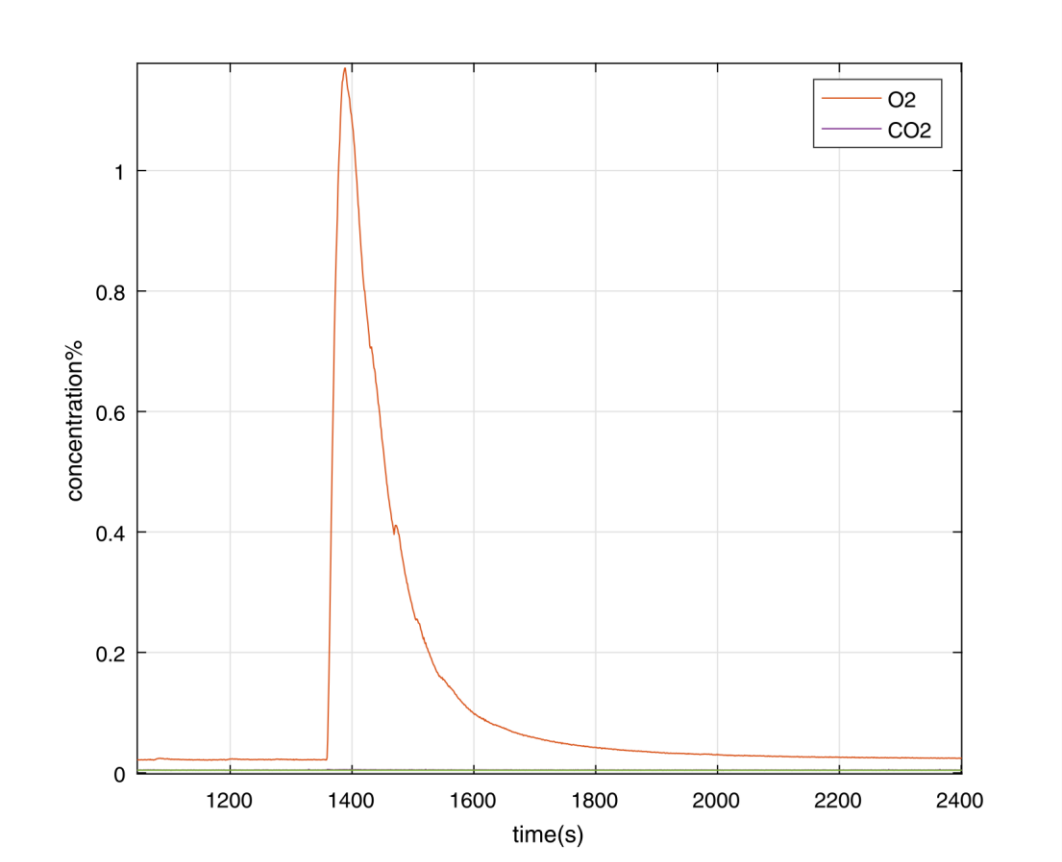

Fig.6. MS data for the evolution of O_2 from Li_2O_2 with 20mM aqueous $FeCl_3$.

Here we can see in Fig.6, the successful evolution of O_2 from the decomposition of Li_2O_2 with aq.$FeCl_3$ based on the Kremer-Stein mechanism. We tried to optimize the concentration of $FeCl_3$. We found out that the O_2 evolution from Li_2O_2 is independent of the concentration as the $FeCl_3$ functions as a catalyst. The quantitative evolution of O_2 occurred with all the tested concentration of aq.$FeCl_3$ was almost the same (Table.1.)

Table.1.Showing the no: of moles of Li_2O_2 that is expected and O_2 evolved from different amounts of Li_2O_2 with different concentrations of aqueous $FeCl_3$.

Conc. of aq.$FeCl_3$ (M)	No: of moles of Li_2O_2 expected	O_2 evolved (in moles)	% of O_2 evolved
0.05	2.569×10^(-5)	1.23×10^(-5)	95.82
0.1	1.725×10^(-5)	8.63×10^(-6)	100.00
0.5	2.019×10^(-5)	9.97×10^(-6)	98.75
1	2.349×10^(-5)	1.19×10^(-5)	101.21

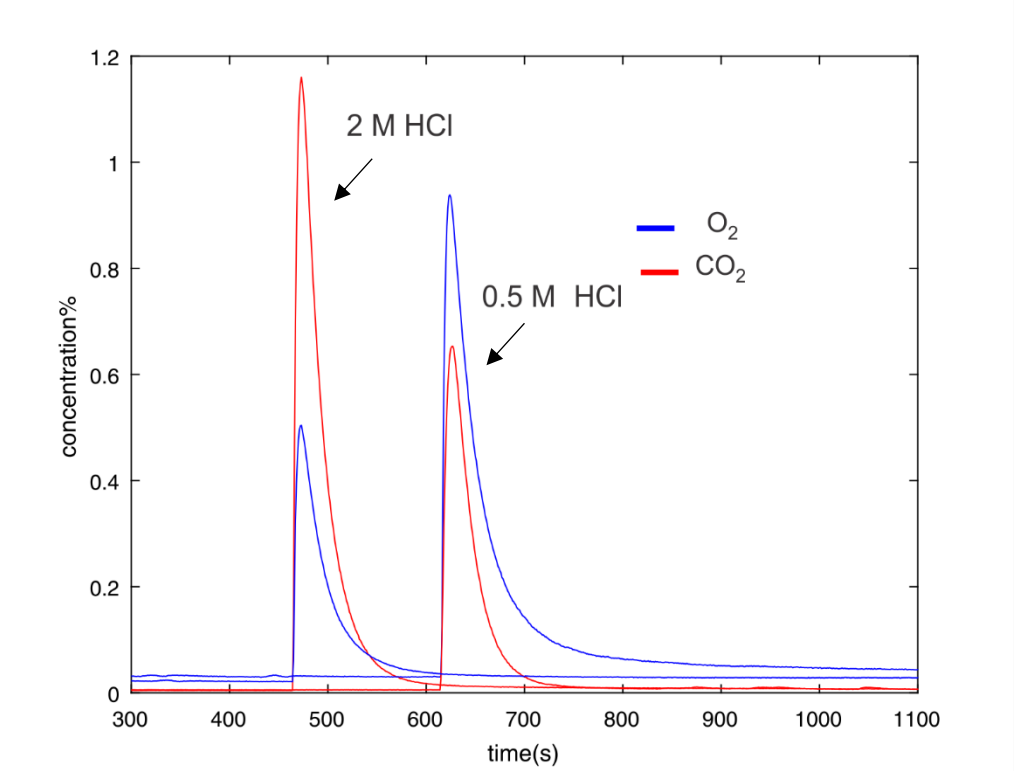

Fig.7. MS data for the evolution of O_2 and CO_2 from Li_2O_2 and Li_2CO_3 respectively in the presence of 20 mM $FeCl_3$ with extra 0.5 M and 2 M HCl.

In order to evolve the inorganic CO_2 along with the O_2, we added acid into the aqueous $FeCl_3$ solution. The addition of extra amount of acid adversely affect the O_2 evolution. As

we can see in Fig.7, the presence of extra acid helps in the successful evolution of CO_2 from the Li_2CO_3.As the concentration of acid increases from 0.5 M to 2 M, it badly affects the O_2 evolution.

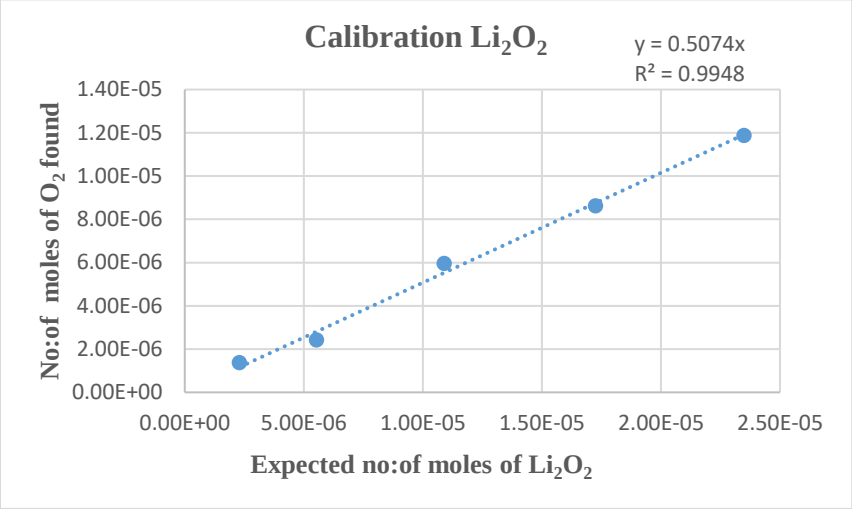

Fig.8. Showing the calibration plot of Li_2O_2.

Table.2.Showing the no: of moles of O_2 evolved from different amounts of Li_2O_2

Amount of Li_2O_2 (mg)	**0.1 M $FeCl_3$ (ml)**	**No: of moles of Li_2O_2 expected**	**No: of moles of O_2 found**	**% of O_2 evolved**
0.1	0.2	2.301×10^(-6)	1.38×10^(-6)	119.62
0.2	0.2	5.544×10^(-6)	2.42×10^(-6)	87.42
0.5	0.2	1.09×10^(-5)	5.96×10^(-6)	109.2
0.7	0.2	1.725×10^(-5)	8.63×10^(-6)	100.00
1	0.2	2.349×10^(-5)	1.19×10^(-5)	101.2

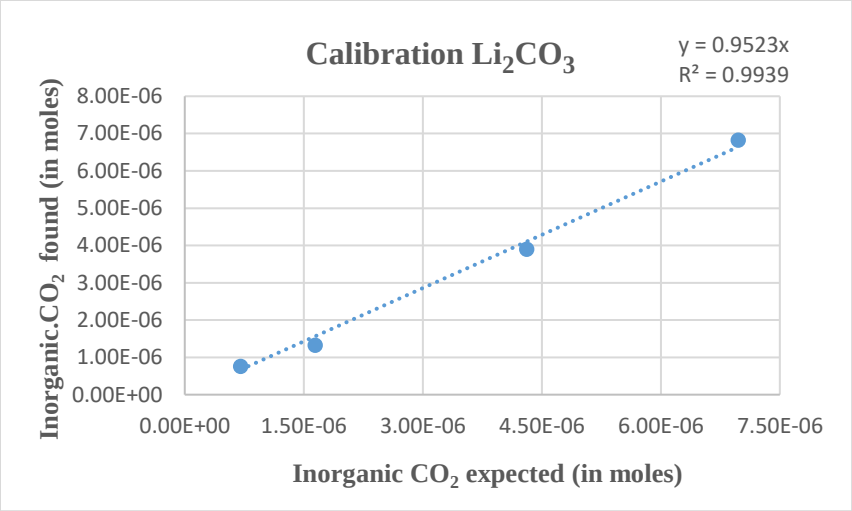

Fig.9. Showing the calibration plot of Li_2CO_3.

Table.3.Showing the no: of moles of CO_2 that is expected and evolved from different amounts of Li_2CO_3.

Amount of Li_2CO_3 (mg)	**2 M H_3PO_4 (ml)**	**Inorg.CO_2 expected (in moles)**	**Inorg.CO_2 found (in moles)**	**% of CO_2 evolved**
0.05	0.2	7.055×10^(-7)	7.59×10^(-7)	107.61
0.1	0.3	1.644×10^(-6)	1.32×10^(-6)	80.33
0.3	0.2	4.311×10^(-6)	3.90×10^(-6)	90.42
0.5	0.2	6.978×10^(-6)	6.82×10^(-6)	97.76

The calibration plots of Li_2O_2 (Fig.8.) and Li_2CO_3 (Fig.9.) help us to determine the amount of Li_2O_2 and Li_2CO_3 in a battery after the discharge. The discharge product along with the side products can be quantitatively determined using this method. Similarly, the organic side product (HCOOLi) can be analysed with the help of $KMnO_4$ as shown below (Fig.10.). We have successfully been able to determine the amount of organic CO_2 from the decomposition of HCOOLi when treating it with 0.5 M $KMnO_4$.

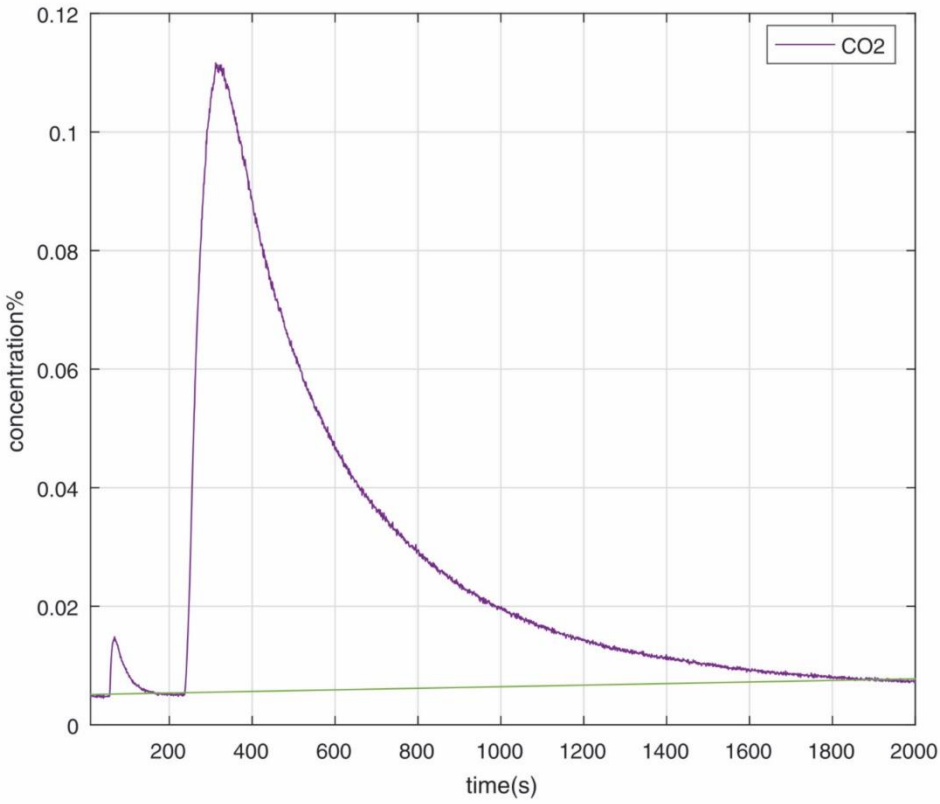

Fig.10. MS data for the evolution of CO_2 from the decomposition of HCOOLi with 2 M H_3PO_4 and 0.5 M $KMnO_4$.

Table.4.Showing the no: of moles of CO_2 that is expected and evolved from different amounts of HCOOLi in the presence and absence of $MnCl_2$.

Amount of HCOOLi (mg)	**Amount of $MnCl_2$ (mg)**	**2 M H_3PO_4 (ml)**	**0.5 M $KMnO_4$ (ml)**	**Org.CO_2 expected(in moles)**	**Org.CO_2 found (in moles)**	**% of Org.CO_2 evolved**
0.119	0	0.1	0.1	2.29×10^(-6)	2.82×10^(-6)	122.78
0.101	4.5	0.1	0.1	1.96×10^(-6)	2.11×10^(-6)	107.74
0.110	4.7	0.1	0.1	2.13×10^(-6)	2.54×10^(-6)	118.77

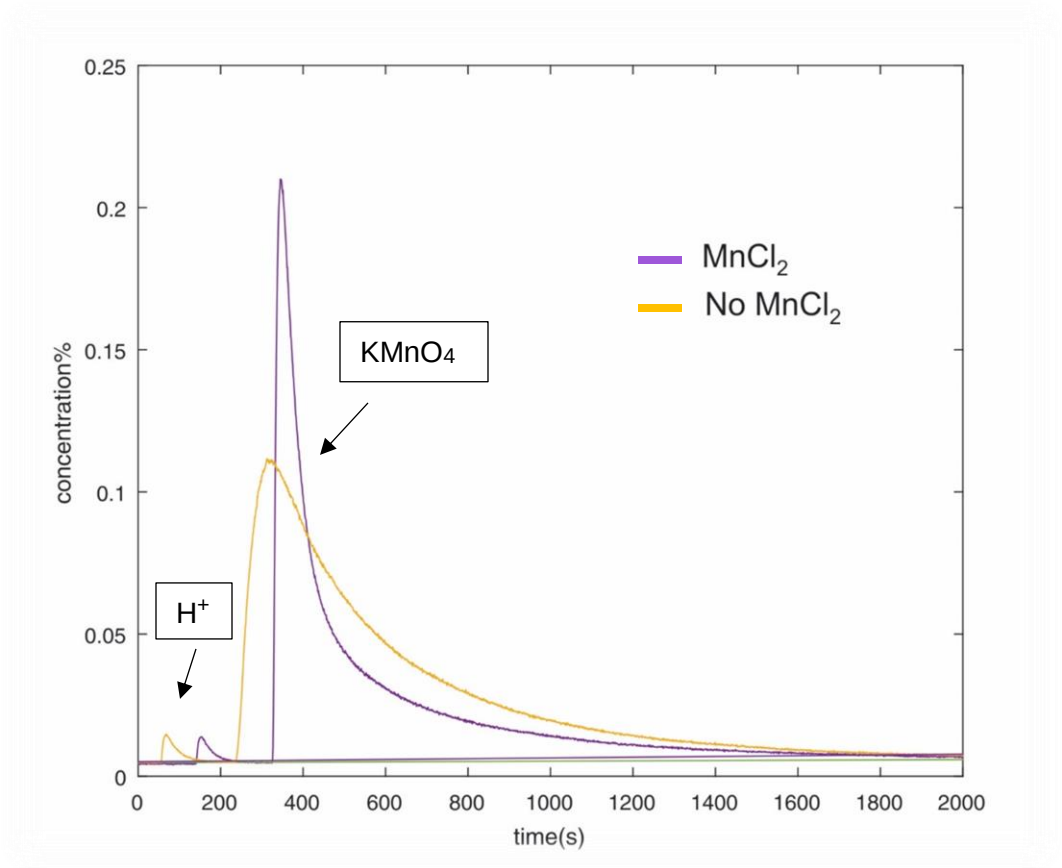

Fig.11. MS data for the evolution of CO_2 from the decomposition of HCOOLi with 2 M H_3PO_4 and 0.5 M $KMnO_4$ in the presence and absence of $MnCl_2$.

It was seen clearly in Fig.11.that the presence of $MnCl_2$ enhances the % concentration of CO_2.The presence of $MnCl_2$ can activate more carbonates species and makes the $KMnO_4$ oxidation much more easily i.e. more CO_2 are generated in a shorter time scale. This we can see clearly in Table.4.that there is not much difference in the CO_2 evolved but the reaction becomes quicker when adding $MnCl_2$.

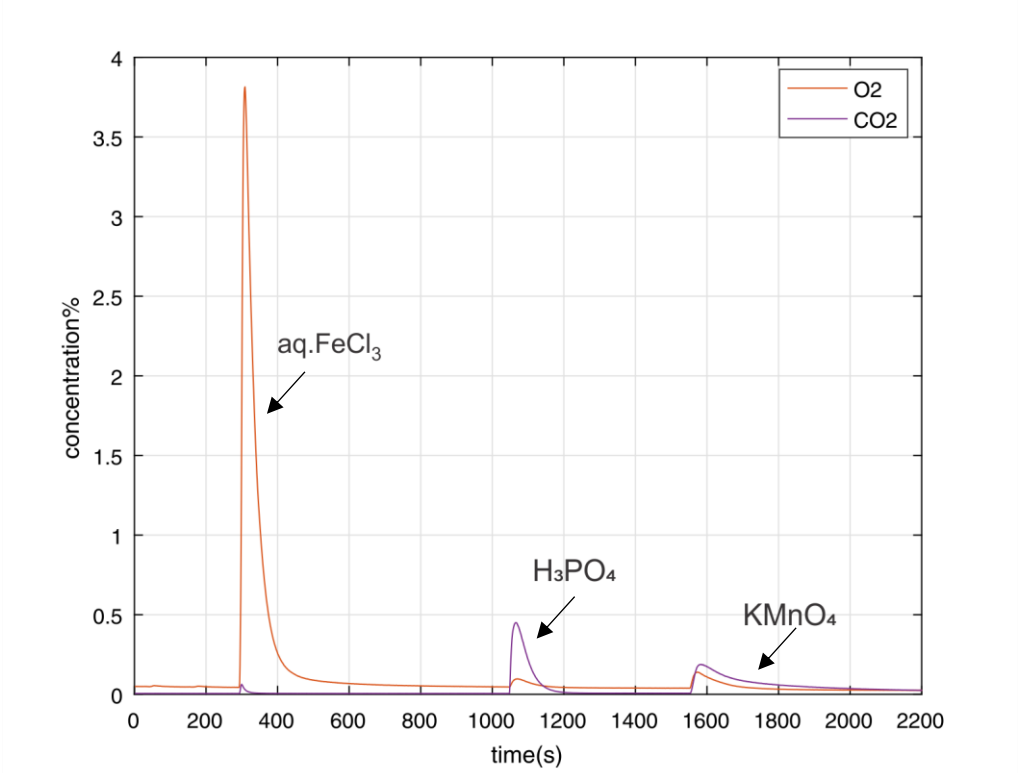

Fig.12. MS data for the evolution of O_2,inorganic and organic CO_2 from Li_2O_2, Li_2CO_3 and HCOOLi with 0.1 M $FeCl_3$,0.5 M $MnCl_2$ in 2 M H_3PO_4 and 0.5 M $KMnO_4$ in 2M H_3PO_4.

The successful evolution of all the expected O_2, inorganic and organic CO_2 occurred during the addition of aq.$Fecl_3$, H_3PO_4 and $KMnO_4$ (Fig.12). The result found was reproducible (Table.5.).

Table.5.Showing the % of O_2, inorganic and organic CO_2 that is evolved from the mixture of Li_2O_2, Li_2CO_3 and HCOOLi.

No:	**Compounds used**	**0.1 M $FeCl_3$(ml)**	**% of O_2 evolved**	**2 M H_3PO_4 (ml)**	**% of inorg.CO_2 evolved**	**0.5 M $KMnO_4$ (ml)**	**% of org.CO_2 evolved**
1.	Li_2O_2,Li_2CO_3,HCOOLi	0.1	99.16	0.1	108.19	0.1	99.02
2.	Li_2O_2,Li_2CO_3,HCOOLi	0.1	99.22	0.1	101.92	0.1	105.03

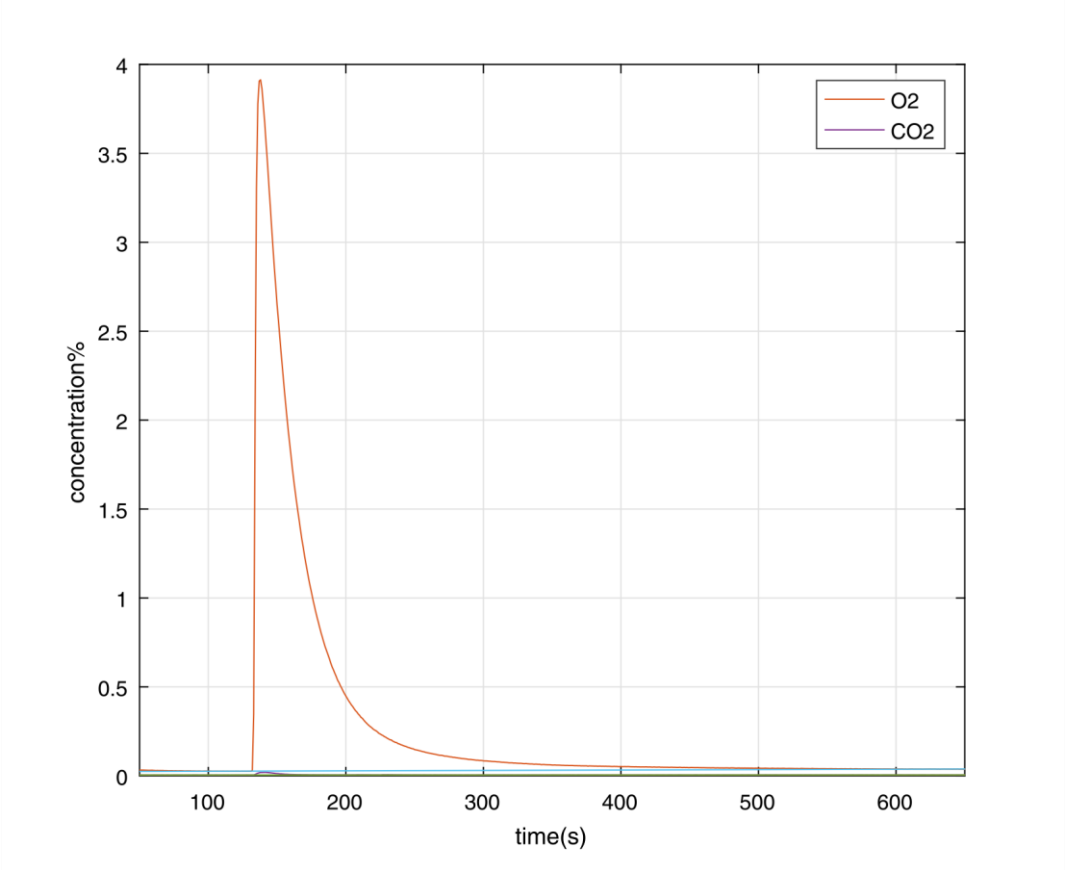

Fig.13. MS data for the evolution of O_2 from KO_2 with 0.1 M $FeCl_3$

In order to test this method for Na-O_2 battery, we took KO_2 as an alternative superoxide for NaO_2.Fig.13 shows the quantitative O_2 evolution from KO_2 with aq.$FeCl_3$.And we have also tried to determine the CO_2 evolution from sodium acetate along with O_2 from KO_2 because it is one of the side product formed during the discharge of Na-O_2 battery. But with permanganometric oxidation, we failed to determine the quantitative amount of sodium acetate (Fig.14) unlike in case of HCOOLi. We found out that the $KMnO_4$ oxidation method is strong enough to evolve the carbonyl carbon but not the alkyl carbons next to it.Table.6 shows the % of O_2 evolution from KO_2.

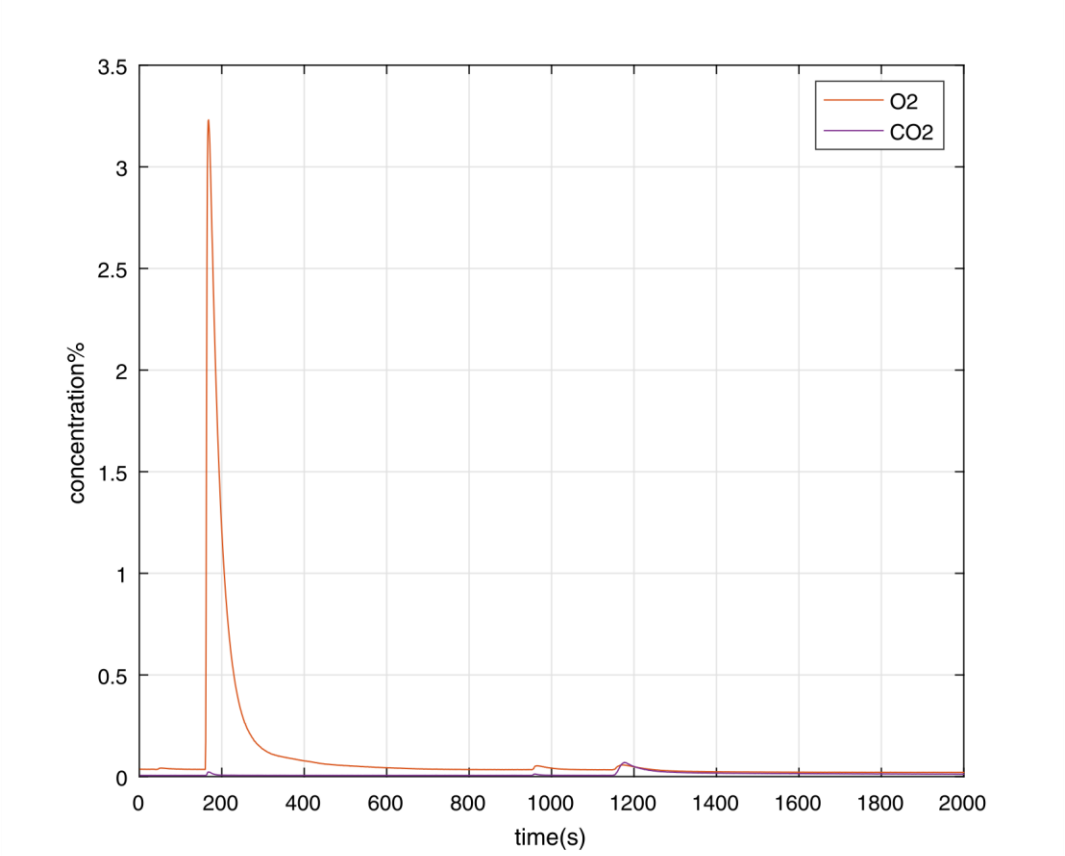

Fig.14. MS data for the evolution of O_2 and CO_2 from KO_2 and NaOAc with 0.1 M $FeCl_3$, 0.5 M H_3PO_4 and 0.5 M $KMnO_4$.

Table.6.Showing the % of O_2 that is evolved from KO_2.

No:	Compounds used	0.1 M $FeCl_3$(ml)	% of O_2 evolved
1.	KO_2	0.1	90.11
2.	KO_2	0.1	90.23
3.	KO_2	0.1	93.44

Since the $KMnO_4$ oxidation failed to work in case of NaOAc, we tried the Fenton's reaction to quantitatively evolve the CO_2 from the organic side products. With the Fenton's reaction, the organic side products generated in the metal-air batteries were successfully quantified as shown below in Fig.15.Even though we found that the quantification of organic side products can be done by this method there are many factors still to be understood like the cross reactivity of different ions in the solution, pH etc. The evolution

of CO_2 from the organic side product decreases due to the presence of $FeCl_3$ in the solution. The quantitative O_2 evolution from Li_2O_2 occurs during the addition of aq.$FeCl_3$ but at the same time, this results in the formation of some radical species which can react with the organic side products and evolve CO_2.So in the Li-air batteries, we can give the total carbon content and the amount of the discharge product.

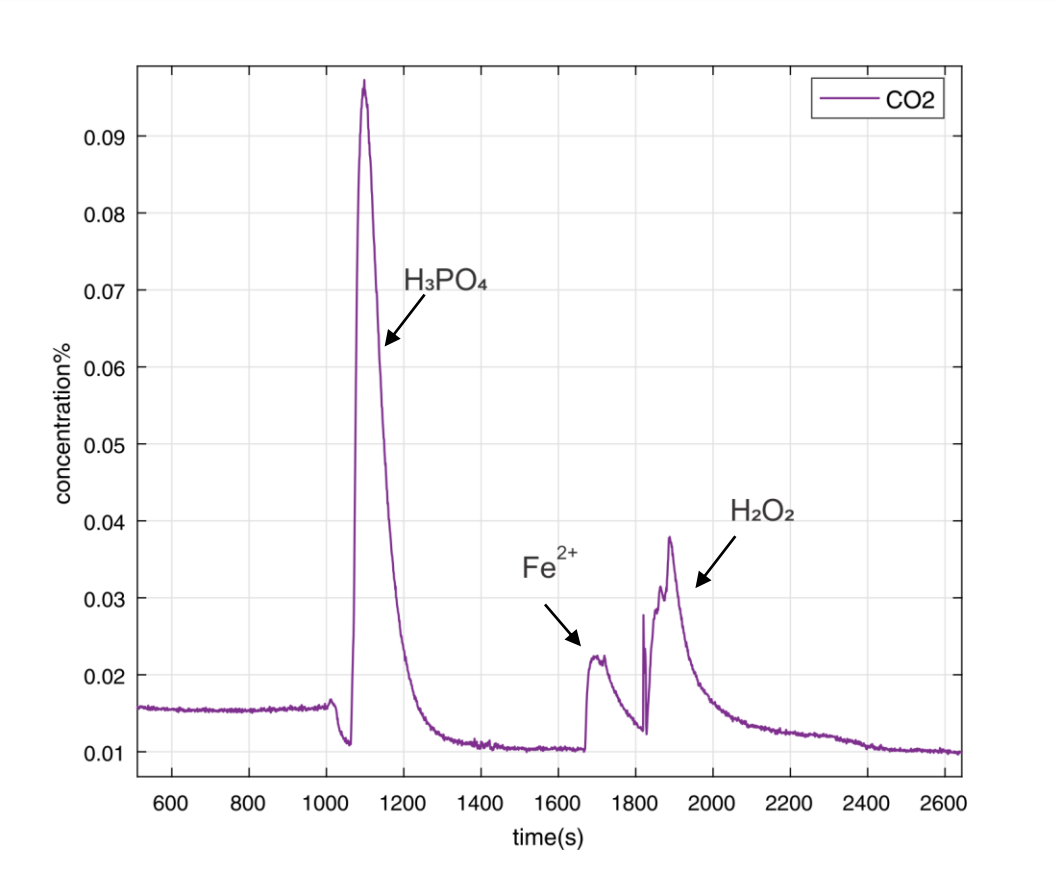

Fig.15. MS data for the evolution of CO_2 from Li_2CO_3 and NaOAc with the Fenton's reagent.

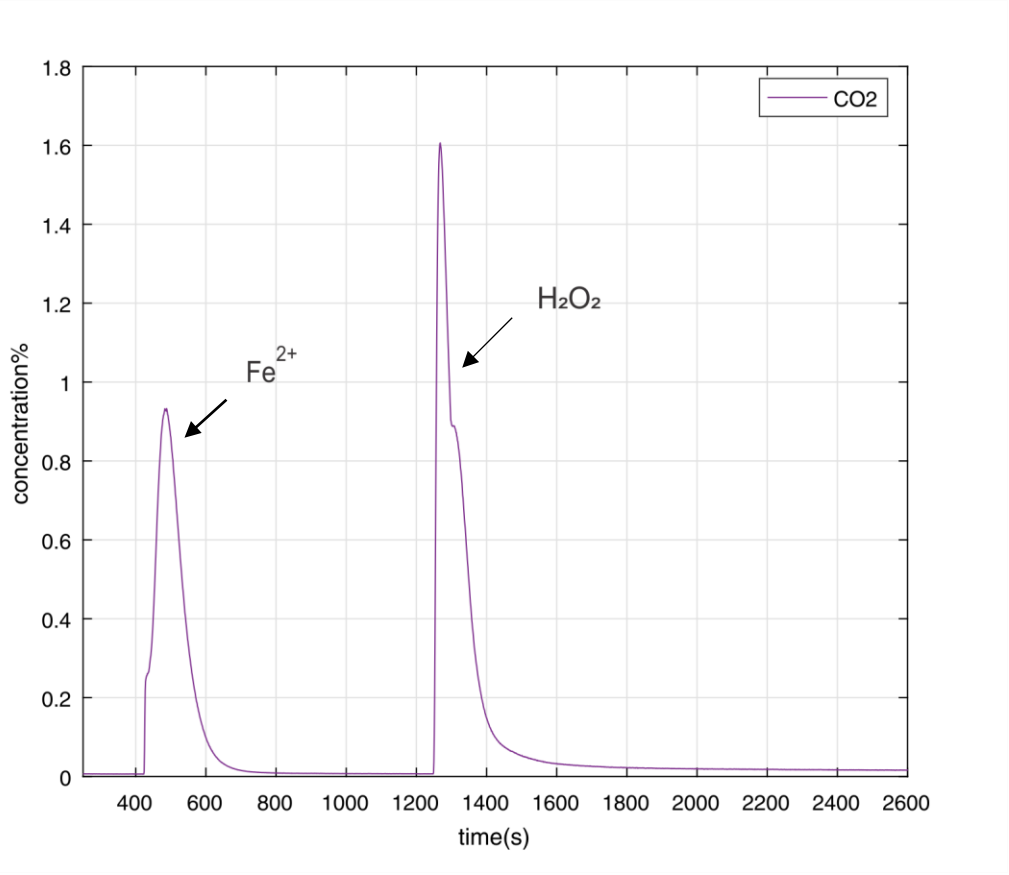

Fig.16. MS data for the evolution of CO_2 from a Li-ion Battery with the Fenton's reagent.

Table.7. Showing the no: of moles of inorganic and organic CO_2 evolved from a Li-ion battery.

Graphite electrode	**$FeSO_4$ in 20% H_3PO_4 (ml)**	**30% H_2O_2 (ml)**	**Inorg.CO_2 evolved (in moles)**	**Org.CO_2 evolved (in moles)**
1.	0.3	0.3	7.36×10^(-6)	1.14×10^(-5)
2.	0.3	0.3	5.46×10^(-6)	7.07×10^(-6)

Then we tried this method in a Li-ion battery since it is the widely accepted energy storage in the current world. The signals from real electrode can be seen in Fig.16. We quantitatively determine the side products generated during the discharge with the Fenton's reagent and the no: of moles of CO_2 evolved from it was shown in Table.7. We have also checked the blank electrodes to make sure that there is no reaction occur between the Graphite electrode and the analysis solutions.

Conclusion

Several pressure measurements were carried out in different solvents like DME and DMSO to measure the no: of electrons per mole of O_2 upon cycling indicates the occurrence of disproportionation reaction ($2\ LiO_2 \longrightarrow Li_2O_2 + O_2$) during the charging of a Li-O_2 battery. To get a better understanding of the impact of the electrolyte on the charging process, a numerical model to separate the faradic and capacitative current has to be developed. In order to quantify the discharge products and the carbonaceous side products generated in a Li-O_2 and Na-O_2 batteries, a method based on Mass Spectrometry has been developed. The quantitative determination of the discharge product was done with aq.$FeCl_3$ and the side products were analysed with H_3PO_4 and the Fenton's reagent. We found that the method works in principle but there are still many factors to be understood especially the cross-reactivity of the ions in the solutions, pH etc.

References

1. Lim, H-D., Lee, B., Cho, K., Kang, K. *Nature Energy*. **2016**, *16066*, 1-9.
2. Knudsen,K.B.; Vegge, T.; McCloskey, B. D.; Hjelm, J. *J. Electrochem.Soc.* **2016**, *163*, A2065-A2071.
3. Abraham, K.M. *J.Electrochem.Soc*.**1996**, *143*, 7.
4. McCloskey, B. D., Luntz, A.C. *J.Am.Chem.Rev.***2014**, *114*, 11721-11750.
5. Aurbach, D., McCloskey, B.D., Nazar, L.F. & Bruce, P.G. *Nature Energy.* **2016**, *16128*.
6. Bruce. P.G, Freunberger, S.A, Hardwick, L.J & Tarascon, J.M. *Nat.Materials*.**2012**, *11*, 19-29.
7. Choi, J.W, Aurbach, D. *Nat. Materials Reviews*.**2016**, *1*.
8. McCloskey, B. D., Bethune, D. S., Shelby, R. M., Girishkumar, G. & Luntz, A. C. *J. Phys. Chem. Lett*. **2011**, *2,* 1161-1166.
9. Peng, Z, Freunberger, S.A, Hardwick, L.J & Tarascon, J.M, Bruce. P.G. *Angew. Chem. Int. Ed.* **2011**, *50*, 6351-6355.
10. Girishkumar, G., McCloskey, B. D., Luntz, A.C., Swanson, S, Wilcke. W.*J. Phys. Chem. Lett.*, **2010**, *1,* 2193-2203.
11. Chen, Y., Freunberger, S. A., Peng, Z., Fontaine, O. & Bruce, P. G. *Nature Chem*. **2013**, *5,* 489–494.
12. Black, R., Adams, B. & Nazar, L.F. *Adv. Energy Mater*. **2012**, *2,* 801-815.
13. Hartmann, P. *et al*. *Nature Materials*. **2013**, *12,* 228–232.
14. Hartmann, P. *et al*. *Phys. Chem. Chem. Phys*. **2013**, *15*, 11661–11672.
15. Xia, C., Fernandes, R., Nazar. L.F. *J.Am.Chem.Soc.* **2016**.
16. McCloskey, B. D., Luntz, A.C., Garcia, J.M. *J. Phys. Chem. Lett,* **2014**, *5*, 1230-1235.
17. McCloskey, B. D.*et.al*. *J. Phys. Chem. Lett*. **2012**, *3*, 997-1001.
18. Ottakam Thotiyl, M.M.; Freunberger. S.A.; Peng. Z.; Bruce. P.G. *J. Am. Chem.Soc*. **2013**, *135*, 494-500.
19. Peng, Z.; Freunberger, S.A.; Bruce, P.G. *Science*. **2012**, *337*, 563-566.

20. McCloskey, B. D., Brunet. A., *J. Phys. Chem. Lett*. **2013**, *4*, 276-279.
21. Ottakam Thotiyl, Freunberger, et al., *Nature Mater.* **2013**, *12*, 1050.
22. McCloskey, B. D. *et al*. *J. Phys. Chem. Lett.* **2013**, *4*, 2989–2993.
23. Chen, Y., Freunberger, S. A., Peng, Z., Barde, F. & Bruce, P. G. *J. Am. Chem. Soc.* **2012***, 134*, 7952–7957.
24. Freunberger, S. A., Chen, Y., Peng, Z., Griffin, J.M., Hardwick. L.J., Barde, F. & Bruce, P. G. *J. Am. Chem. Soc.* **2011**, *133*, 8040-8047.
25. Veith, G.M., Nanda. J., Delmau, L.H., Dudney, N.J. *J. Phys. Chem. Lett.* **2012**, *3*, 1242-1247.
26. Kremer, M. L. *Trans Faraday Soc*.**1963**, *59*, 2535.
27. Kremer, M. L., Stein, G. *Int. J. Chem. Kinetics*. **1977**, *9*, 179-184.
28. Chin, D-H., Chiericato, Nanni, E.J., Sawyer, D.T. *J. Am. Chem. Soc.* **1982**, *104*, 1296- 1299.
29. Hartmann, P., Grubl, D., Sommer, H., Janek, J., Bessler, W.G., Adelhelm, P. *J. Phys. Chem. C.***2014**, *118*, 1461-1471.
30. Tarascon, J-M., Larcher, D., Grimaud, A., Lepoivre, F. *J. Electrochem.Soc.* **2016**, *163*, A923-A929.